Light induced self-written waveguides interactions in photopolymer media

Mohamed Ben Belgacem,[1,2] **Saber Kamoun,**[1] **Mohamed Gargouri,**[1] **Kokou D. (Honorat) Dorkenoo,**[2] **Alberto Barsella,**[2] **and Loïc Mager**[2,*]

[1]*Laboratoire de l'État Solide, Groupe Télécommunication Optique, Faculté des Sciences de Sfax, B.P. 1171, 3000 Sfax, Tunisia*
[2]*Institut de Physique et Chimie des Matériaux de Strasbourg (IPCMS), UMR7504, CNRS-Universite de Strasbourg, 23 rue du Loess, B.P. 43, 67034 Strasbourg CEDEX 2, France*
[*]*loic.mager@ipcms.unistra.fr*

Abstract: We present experimental and theoretical study of the interaction of Light Induced Self-Written (LISW) waveguides in photopolymers. We show that the diffusion of the monomer controls the refractive index distribution. Consequently it influences the interaction between the LISW channels allowing the observation of anti-crossing behavior or the propagation of an array of non interacting LISW waveguides.

© 2015 Optical Society of America

OCIS codes: (160.5320) Photorefractive materials; (310.2790) Guided waves; (190.6135) Spatial solitons; (130.5460) Polymer waveguides.

References and links

1. S. J. Frisken, "Light-induced optical waveguide uptapers," Opt. Lett. **18**, 1035–1037 (1993).
2. K. Yamashita, M. Ito, E. Fukuzawa, H. Okada, and K. Oe, "Device Parameter Analyses of Solid-State Organic Laser Made by Self-Written Active Waveguide Technique," J. Lightwave Technol. **27,** 4570–4574 (2009).
3. S. Kamoun, A. Jemal, M. Gargouri, A. Barsella, L. Mager, H.I.E. Arach, K.D. Dorkenoo, and A. Fort, "Filamentation-free self-written waveguides in a photopolymerizable medium initiated by multimode optical fibers," Appl. Optics **49**, 2095-2098 (2010).
4. K.D. Dorkenoo, O. Crégut, L. Mager, F. Gillot, C. Carre, and A. Fort, "Quasi-solitonic behavior of self-written waveguides created by photopolymerization," Opt. Lett. **27**, 1782–1784 (2002).
5. G. Zhao and P. Mouroulis, "Diffusion Model of Hologram Formation in Dry Photopolymer Materials," J. Mod. Optics **41**, 1929–1939 (1994).
6. J.T. Sheridan, M. Downey, and F. T. ONeill, "Diffusion-based model of holographic grating formation in photopolymers: generalized non-local material responses," J. Opt. A-Pure Appl. Op. **3**, 477-488 (2001).
7. T. Babeva, I. Naydenova, S. Martin, and V. Toal, "Method for characterization of diffusion properties of photopolymerisable systems," Opt. Express **16**, 8487-8497 (2008).
8. T. M. Monro, C. M. Sterke, and L. Poladian, "Self-writing waveguide in glass using photosensitivity," Opt. Commun. **119**, 523-526 (1995).
9. T.M. Monro, C.M. Sterke, and L. Poladian, "Catching light in its own trap," J. Mod. Optic **48**, 191–238 (2001).
10. T. Yamashita and M. Kagami, "Fabrication of Light-Induced Self-Written Waveguides With a W-Shaped Refractive Index Profile," J. Lightwave Technol. **23**, 2542–2548 (2005).
11. A. Zohrabyan, A. Tork, R. Birabassov, and T. Galstian, "Self-written gradient double claddlike optical guiding channels of high stability," Appl. Phys. Lett. **91**, 111912 (2007).
12. T. Babeva, I. Naydenova, S. Martin, and V. Toal, "Method for characterization of diffusion properties of photopolymerisable systems," Opt. Express **16**, 8487–8497 (2008).
13. T. Babeva, D. Mackey, I. Naydenova, S. Martin, and V. Toal, "Study of the photoinduced surface relief modulation in photopolymers caused by illumination with a Gaussian beam of light," J. Opt. **12**, 124011 (2010).
14. K.D. Dorkenoo, F. Gillot, O. Crégut, Y. Sonnefraud, A. Fort, and H. Leblond, "Control of the Refractive Index in Photopolymerizable Materials for (2+1)D Solitary Wave Guide," Phys. Rev. Lett. **93**, 143905 (2004).
15. W. Heller, "Remarks on refractive index mixture rules," J. Phys. Chem. **69**, 1123–1129 (1965).

16. P. Ho and Y. Lu, "Improving the beam propagation method for TM polarization," Opt. Quant. Electron. **35**, 1–14 (2003).
17. S. Gallego, A. Márquez, M. Ortuño, J. Francés, S. Marini, A. Beléndez, and I. Pascual, "Surface relief model for photopolymers without cover plating," Opt. Express **19**, 10896–10906 (2011).
18. K. Shojiro and N. Shigeo, "Characteristics of a doubly clad optical fiber with a low-index inner cladding," IEEE J. Quantum Elect. **10**, 879–887 (1974).
19. G. I. Stegeman and M. Segev, "Optical spatial soliton and their interaction: Universality and diversity," Science **286**, 1518–1525 (1999).
20. T. Yoshimura and H. Kaburagi, "Self-Organization of Coupling Optical Waveguides by the 'Pulling Water' Effect of Write Beam Reflections in Photo-Induced Refractive-Index Increase Media," Proc. SPIE **7221**, 722111 (2009).
21. S. Shoji, S. Kawata, A.A. Sukhorukov, and Y.S. Kivshar, "Self-written waveguides in photopolymerizable resins," Opt. Lett. **27**, 185–187 (2002).
22. C. Jisha, V. Kuriakose, and K. Porsezian, "Dynamics of a light induced self-written waveguide directional coupler in a photopolymer," Opt. Commun. **281,** 1093–1098 (2008).
23. A. Jemal, M. Ben Belgacem, S. Kamoun, M. Gargouri, K.D.H. Dorkenoo, A. Barsella, and L. Mager, "Electro-optic phase modulation in light induced self-written waveguides propagated in a 5CB doped photopolymer," Opt. Express **21**, 1541–1546 (2013).
24. K. Yamashita, M. Ito, E. Fukuzawa, H. Okada, and K. Oe, "Device Parameter Analyses of Solid-State Organic Laser Made by Self-Written Active Waveguide Technique," J. Lightwave Technol. **27**, 4570–4574 (2009).
25. O. Sugihara, S. Yasuda, B. Cai, K. Komatsu, and T. Kaino, "Serially grafted polymer optical waveguides fabricated by light-induced self-written waveguide technique," Opt. Lett. **33** 294–296 (2008).

1. Introduction

Since the demonstration of the fabrication of Light Induced Self-Written (LISW) waveguides in photopolymers [1] they are no more limited to fundamental studies but foreseen for effective applications. The versatility of this technique allows the elaboration of complex 3D cellular solids that were only available through photolithographic processes. The LISW guides also find applications for optical integrated systems [2]. They can be used to couple energy from a fiber, a beam to a waveguide and to couple one waveguide to another [3, 4]. In photopolymers, the LISW channels are induced by actinic light propagating in the medium. The light is brought into the material through an optical fiber and the increase of the refractive index provided by the photopolymerization compensates the diffraction leading to a quasi-solitonic propagation of the light in the material. The track of the light remains even after the full curing of the material constituting a permanent optical waveguide.

The initial photopolymer mixture can be simply composed of a monomer and photoinitiator. When the photopolymerizable material is exposed to a non uniform illumination, like a interference pattern [5, 6] or a Gaussian light distribution [7], the photopolymerization rate is greater in the bright region than in the dark region. This non-uniform irradiation distribution gives rise to monomer concentration gradients and therefore diffusion of monomers from dark regions to the neighboring bright regions. Likewise in LISW guide propagation, as the light distribution is particularly non uniform, one expects some influence of the monomer redistribution.
In this paper, we present an experimental and theoretical study the interaction of LISW waveguides in photopolymers that evidences the influence of the diffusion.

2. Model

Various phenomenological models have been proposed for the photopolymerization to account for the observation of refractive index modulation in different materials. All the models assume that the refractive index increases monotonically upon actinic illumination. The phenomenological formulation for the evolution of refractive index in LISW propagation is simply expressed as [8, 9]: $d\Delta n/dt = A_p I(1 - \Delta n/\Delta n_s)$ where A_p is a real coefficient depending upon material properties, I is the actinic light intensity, t is the time, and Δn_s is the maximum refractive index change. But such an expression is unable to describe the non monotonic refractive index

variations observed in different LISW channel propagation experiments [10, 11]. To explain the observed W-shaped refractive index profile, one calls upon the role of the redistribution of individual components in the material. Because of the non uniform photopolymerization, the individual optical and diffusion properties of the different chemical species lead to a more complex variation of the index profile.

The effect of the diffusion has already been considered in the Photopolymerization Driven Diffusion (PDD) model proposed by Zaho and al. [5] describing the evolution of monomer fraction under a sinusoidal illumination. The description of the evolution of the material takes into account the diffusion and the photopolymerization. This model has been generalized by Sheridan and al. [6] to non sinusoidal light distribution and allows the computation of refractive index evolution. For the LISW channel initiated from a Gaussian illumination profile, we implement the PDD model to describe the material's response during the propagation introducing a saturation term. This term is required to account for the bleaching of the photo-initiator and the accompanying decrease of the absorption during the photopolymerization. The evolution is then described by two equations, representing the volume fraction of the monomer M and the polymer P:

$$\frac{\partial M(r,t)}{\partial t} = \nabla \cdot (D \nabla M(r,t)) - K_{\mathrm{R}} \cdot M(r,t) \cdot I(r,t) \cdot \left(1 - \frac{\Delta n(r,t)}{\Delta n_{\mathrm{f}}} \right) \tag{1}$$

$$\frac{\partial P(r,t)}{\partial t} = K_{\mathrm{R}} \cdot M(r,t) \cdot I(r,t) \cdot \left(1 - \frac{\Delta n(r,t)}{\Delta n_{\mathrm{f}}} \right) \tag{2}$$

The first term of Eq. (1) describes the diffusion of monomer with its diffusion coefficient D. The second term describes the temporal evolution of the polymer with its polymerization rate K_{R} in both equations, I is intensity of light, $(1 - \Delta n / \Delta n_{\mathrm{f}})$ expresses the saturation and acts as the bleaching term, $\Delta n = n - n_{\mathrm{m}}$ with n the index of refraction of the mixture and n_{m} that of the monomer, $\Delta n_{\mathrm{f}} = n_{\mathrm{p}} - n_{\mathrm{m}}$ with n_{p} the index of refraction of the polymer. Rigorously, the diffusion of monomer changes as polymerization proceeds and the smaller polymer chains can diffuse away from the site of their formation [12, 13]. However, in our experiment, the material undergoes a first uniform photopolymerization stage before the propagation of the LISW channel to reduce the final refractive index modulation and insure stable propagation of the induced waveguide [14]. Accordingly, we consider that the volume fraction of monomer is much lower than that of the polymer. For the same reasons, we assume that the diffusion coefficient of the monomer is constant and negligible for the polymer, as its size and its molecular weight are much larger than that of the monomer. To take into account the variation of the monomer and polymer concentrations, the refractive index of the mixture is calculated from the refractive index of the individual components considering the molecular linear polarizabilities via Lorentz-Lorenz relation [15]:

$$\frac{n^2 - 1}{n^2 + 2} = M \frac{n_{\mathrm{m}}^2 - 1}{n_{\mathrm{m}}^2 + 2} + P \frac{n_{\mathrm{p}}^2 - 1}{n_{\mathrm{p}}^2 + 2} + A \frac{n_{\mathrm{a}}^2 - 1}{n_{\mathrm{a}}^2 + 2} \tag{3}$$

where n_{a} and A are respectively the refractive index and volume fraction of any other chemical specie that does not undergo any modification during the photopolymerization process (e.g. dye, co-initiator, liquid crystal...). A is calculated from the conservation of the total volume fraction: $A = 1 - P - M$.

The simulation of the propagation of the LISW guide is achieved through a temporal loop. We start from the initial uniformly distributed volume fraction of monomer M_i and polymer P_i. The light distribution is computed via a beam propagation method (BPM) [16] solving the Helmholtz equation in the paraxial approximation:

$$j\frac{\partial \psi}{\partial z} + \frac{1}{2k_0}\nabla_{\perp}^2 \psi + \frac{1}{2}k_o\left(\frac{n^2}{\bar{n}^2} - 1\right)\psi = 0, \tag{4}$$

where z is direction of propagation, ψ is the electric field amplitude, k_0 is the a wave vector, n is the spatially-dependent refractive index and $\bar{n}$ is the average refractive index of the propagation medium. The light intensity is calculated from ψ and the monomer and polymer distribution are actualized using Eqs. (1)–(2). The refractive index n variation is calculated from these new concentrations and used to calculate the light distribution in the next time step. The loop is repeated until the end of the simulation. Because of computing capacity and speed limitations, the simulation is performed in a 2D space. We have validated the simulation in 3D through some simulation in a much smaller volume and did observe the same behavior as in 2D.

3. Results and discussion

For the experimental part, we perform our study using a radical photopolymerizable formulation composed by tri-functional acrylate monomer, the pentaerythritoltriacrylate 'PETA' monomer ($\sim$90% wt.), a xanthenic dye sensitizer Eosin Y ($\sim$0.5% wt.) and a co-initiator methyldiethanolamine 'MDEA' ($\sim$9.5% wt.). The mixture is conditioned between two glass plates separated by a 125 μm gap and a single mode optical fiber dipped in the solution. Then, the material undergoes a first uniform photopolymerization induced by exposure for 10 minutes under a white lamp (halogen 20W). The fiber is coupled to an cw argon laser delivering the actinic light at 514 nm to launch the LISW channel inscription. Typical power at the fiber output for the inscription in the prepolymerized material is around 1 μW .
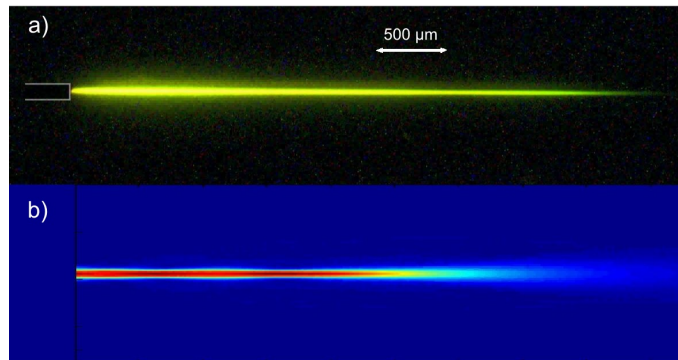

Fig. 1. a) Observation through optical microscopy of the propagation of a LISW waveguide in PETA/Eosin Y/MDEA. b) Simulation of the light distribution of the propagating LISW waveguide. The light is injected from a single-mode optical fiber on the left (Visualization 1).

Figure 1(a) shows the propagation of the self-written guide in the cell observed by optical microscopy. The observation is made very easy as the fluorescence of the unconsumed the Eosin Y decouples from the guide. The refractive index of the MDEA, which is not consumed during the reaction, is equal $n_a = 1.46$. For the PETA monomer the index is $n_m = 1.48$ and after total conversion to polymer it is equal to $n_p = 1.52$. The polymerization rate $K_R = 0.6$ cm$^2/\mu$W and of the diffusion constant $D = 6\cdot 10^{-15}$ m^2/s have been measured experimentally [17]. The detailed description of the experimental process is outside of the scope of this paper and will appear elsewhere.

3.1. Simulation of the propagation of a single LISW waveguide

First, we check that the simulation is able to reproduce the behavior previously observed in LISW channel fabrication experiments [4] [Fig. 1]. In the additional material, we present a video showing simultaneously the experimental observation and the simulation of the LISW channel propagation (see media). As K_R and D have been defined, the different propagation regimes depend on the product of the initial monomer volume fraction and the light intensity $M(r,t) \cdot I(r,t)$. We define the initiating beam as a Gaussian light distribution with a 10 μm diameter at $1/e$ and a $I_0 = 0.5$ mW/cm^2 intensity for all the simulations presented here. Varying only the initial volume fraction of monomer from $M_i = 0.5$ to $M_i = 0.1$, we observe a progressive transition from a chaotic behavior (filamentation) [Fig. 2(a)] to a defined optical channel confining a single propagation mode [Fig. 2(b)].
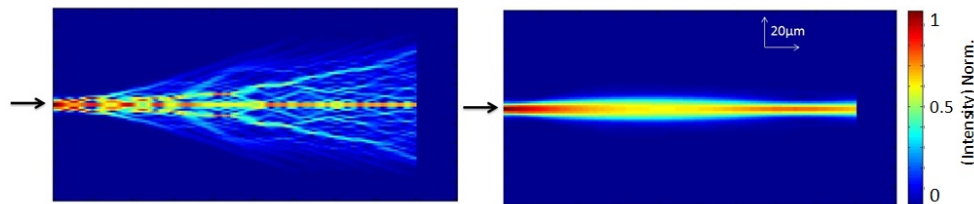

Fig. 2. Simulation of the the light intensity distribution. Effect of the initial monomer fraction on the propagation of the LISW channel propagation a) $M_i = 0.5$, filamentation b) $M_i = 0.1$, single-mode LISW channel propagation. The black arrow shows the direction of the light injection.

The same behavior is observed experimentally [14] increasing the intensity of the seeding beam. The Eqs. (1)–(2) clearly show that the propagation regime LISW guide depends on the $M(r,t) \cdot I(r,t)$ product. Varying the initial monomer concentration affects the propagation regime as well as the initial intensity does. In the simulations, we use the same initial intensity and, considering these previous results, we choose a initial value $M_i = 0.1$ to perform the following simulations. Experimentally, M_i is controlled by the prepolymerization performed under uniform actinic light.

The simulation shows the role of the diffusion of the monomer in determining the distribution of the refractive index [Fig. 3]. In Eq. (1), if $D = 0$ the refractive index variation associated to the construction of the LISW channel is strictly positive [Fig. 3 red line]. When $D \neq 0$ the distribution of the refractive index is more complex [Fig. 3 black line] and especially shows a negative variation at the edge of the guide exhibiting the W-shape experimentally observed [10, 11].

Here the W-shaped profile originates from the propagation and the diffusion, but such index profiles have been designed to increase the mode confinement in silica optical fiber [18]. In the case of the photopolymer considered here, the difference of the refractive index variation with or without the diffusion is of the order of 10^{-3}. Considering this value, the simulation only give a confinement increase of 2% and has not been observed experimentally.

3.2. Counter-propagating LISW waveguides

The LISW waveguides have been considered for the connection of optical fibers. Different groups reported on the interaction of counter-propagating LISW channels initiated from single mode optical fibers. The fusion of the guides allows an efficient connection without strict initial alignment conditions. We perform the simulation of that interaction with seeds separated by a distance of 200 μm and with 10 μm lateral shift as a example of misalignment.
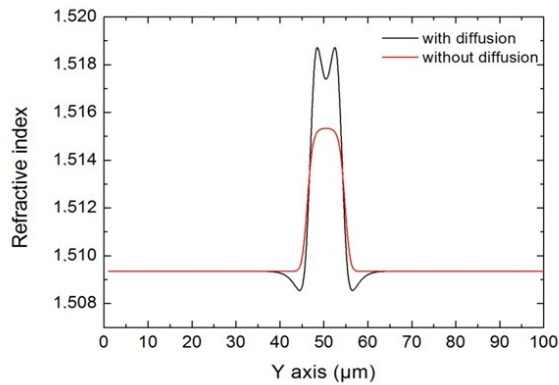
Fig. 3. Simulation of the diffusion effect on the transverse refractive index profile of LISW waveguides. (black line) with diffusion (red line) without diffusion

Our results show that the monomer diffusion and the resulting decrease of the refractive index on the edge of the core of the channel influences the interaction between two LISW waveguides. To demonstrate this influence, we simulate the collision of two LISW guide propagated in opposite directions with an small lateral shift [Figs. 4 and 5]. The simulation shows that fusion occurs when no diffusion of the monomer is allowed ($D = 0$).
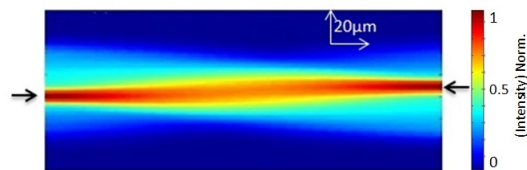
Fig. 4. Simulation of the light intensity distribution. Fusion of two counter-propagating LISW waveguides with a lateral shift of 10μm offset and without diffusion. The black arrows indicate the initial direction of the injected light seed.

When the diffusion is allowed, the simulation leads to an anti-crossing of LISW waveguides [Fig. 5(b)] and to a deviation of the trajectory of the spatial solitons. It is to be noted that the two light field are considered as incoherent as the sum of their intensity is only taken into account for the calculation of the medium evolution.

This anti-crossing of two LISW channels is observed experimentally in PETA/MDEA/Eosin Y formulation. To generate a photopolymer junction in the liquid formulation, we launch two counter-propagating LISW guides from two single mode optical fibers. The fiber outputs face one another at a distance of about 300 μm in a cell as described previously. Because of a slight misalignment of the fibers, we observe an anti-crossing between of the LISW channels [Fig. 6]. Attractive or repulsive interaction between coherent spatial soliton have already been extensively described [19]. In the present experiment, as there is no coherence between the two light fields, this repulsive behavior can be explained by the refraction of the light of one of the guide in a positive index gradient induced by the propagation of the other guide.

Experimentally, the presence of MDEA appears to have an influence on the anticrossing behavior. When replacing the photoinitiating system Eosin Y/MDEA by 5% wt. of Igarcure 784 (CIBA), one observes the fusion of the counter-propagating waveguides. The situation is then
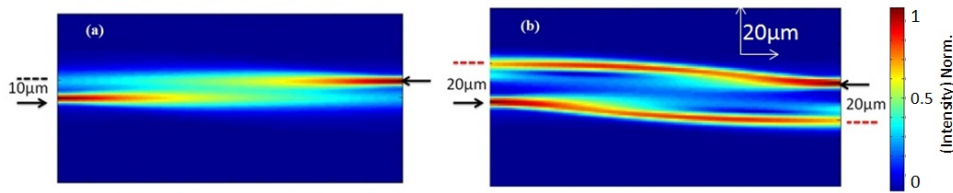
Fig. 5. Simulation of the light intensity distribution. Anti-crossing interaction of two counter-propagating LISW waveguides with a lateral shift of 10 μm offset and with diffusion a) at the beginning of propagation b) end of propagation. The black arrows indicate the initial direction of the injected light seed.
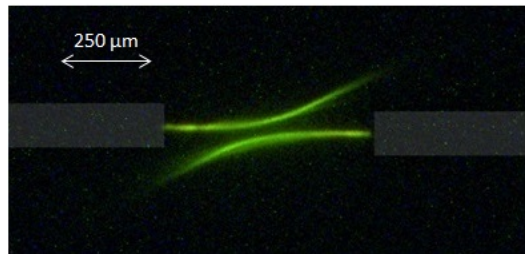

Fig. 6. Observation through optical microscopy of the anti-crossing of counter-propagating LISW waveguides in PETA/Eosin Y/MDEA.

similar to this described in previous work where two counter-propagating are attracted to each other and merge naturally into a single optical path [20]. According to the model the distribution of the MDEA depends on the polymer concentration. Therefore, the MDEA contributes to the induced refractive index gradient. It also acts as a plasticizer and increases the diffusion.

3.3. Propagation of parallel LISW waveguides

In this part our objective is to study the effect of interaction on the propagation of parallel LISW channels. We start with the interaction of just two parallel LISW guides. Figure 7 shows the importance of the distance of separation between the waveguides. If the separation is larger than 20 μm there is no interaction between the waveguides. If we decrease this distance to 10 μm one observes a deviation of the direction of propagation waveguide and we have a repulsive interaction between the two LISW.
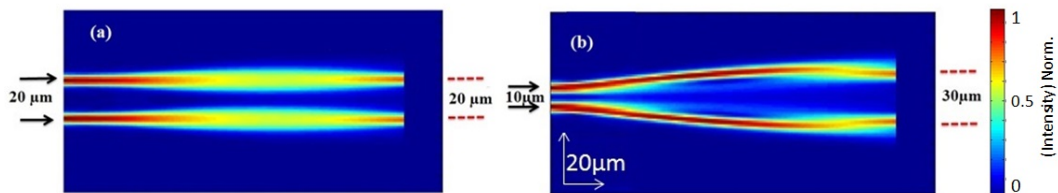

Fig. 7. Simulation of the light intensity distribution. Interaction of two parallel LISW waveguides, a) 20 μm distance: no interaction b)10 μm distance: repulsed interaction.

This interaction is caused by the influence of the monomer diffusion on the beam propagation

and results in the deviation of the waveguide. Now in Fig. 8, when three or five waveguides are propagated simultaneously, we observe that the LISW channel in the middle propagates without deviation because of the combined influences of the surrounding guides. In this case, the repulsive interactions compensate to leave the trajectory of the central waveguide unchanged.
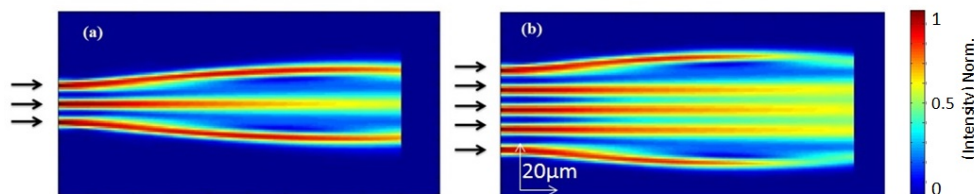

Fig. 8. Simulation of the light intensity distribution. Propagation of multiple parallel LISW waveguides a) 3 waveguides b) 5 waveguides.

This behavior is verified experimentally [Fig. 9], propagating simultaneously many LISW guides in the same solution as described earlier. We observe the parallel propagation of this LISW channel array with no fusion or crossing.
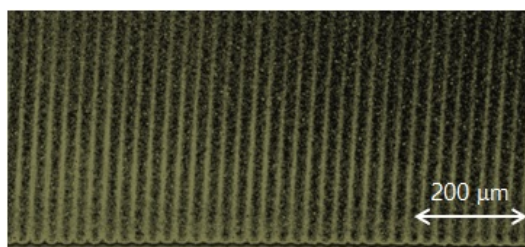

Fig. 9. Observation by optical microscopy of the propagation of multiple parallel LISW waveguides without fusion.

4. Conclusion

We have demonstrated that the diffusion of the monomer has an important influence on the interaction between LISW waveguides. This is especially important to for writing optical components like Y and X junction or a LISW coupler [21, 22]. The addition of a chemical specie for the the implementation of specific optical function: electro-optical [23], fluorescence[24] and photochromic[25], may also plasticize the material and therefore enhance the diffusion. This effect has to be considered in the fabrication of LISW channel based devices. To assist this task, we have developed a model for the material that represents a good trade-off between the simplicity required for the computation and the complexity of a complete model for the photopolymerization. The simulations performed with this model allow a better understanding the construction of LISW optical waveguides and suggests new solutions to control and optimize the self-written channels.